Adhesion and migration of CHO cells on micropatterned single layer graphene

2017 2D Mater. 4 025022

(http://iopscience.iop.org/2053-1583/4/2/025022)

2D Materials

OPEN ACCESS

RECEIVED
12 August 2016

REVISED
6 December 2016

ACCEPTED FOR PUBLICATION
9 January 2017

PUBLISHED
1 February 2017

PAPER

Adhesion and migration of CHO cells on micropatterned single layer graphene

S Keshavan[1], R Oropesa-Nuñez[1], A Diaspro[1,2], C Canale[1] and S Dante[1]

[1] Department of Nanophysics, Istituto Italiano di Tecnologia, Genova, Italy
[2] Department of Physics, University of Genova, Genova, Italy

E-mail: silvia.dante@iit.it **and** sandeep.keshavan@iit.it

Keywords: graphene, patterning, cell adhesion, cell migration, single cell force spectroscopy

Supplementary material for this article is available online

Abstract

Cell patterning technology on single layer graphene (SLG) is a fairly new field that can find applications in tissue engineering and biomaterial/biosensors development. Recently, we have developed a simple and effective approach for the fabrication of patterned SLG substrates by laser micromachining, and we have successfully applied it for the obtainment of geometrically ordered neural networks. Here, we exploit the same approach to investigate the generalization of the cell response to the surface cues of the fabricated substrates and, contextually, to quantify cell adhesion on the different areas of the patterns. To attain this goal, we tested Chinese hamster ovary (CHO) cells on PDL-coated micropatterned SLG substrates and quantified the adhesion by using single cell force spectroscopy (SCFS). Our results indicate higher cell adhesion on PDL-SLG, and, consequently, an initial CHO cell accumulation on the graphene areas, confirming the neuronal behaviour observed previously; interestingly, at later time point in culture, cell migration was observed towards the adjacent SLG ablated regions, which resulted more favourable for cell proliferation. Therefore, our findings indicate that the mechanism of interaction with the surface cues offered by the micropatterned substrates is strictly cell-type dependent.

1. Introduction

In tissue engineering, cell patterning plays a vital role in controlling and guiding cell position to the desired locations. The interplay between physical, chemical and topographical surface cues and the cellular response is the subject of many investigations (Jeon *et al* 2014) and it is well known that surface patterning may affect many cellular processes such as cell-cell communication and migration (Ventre *et al* 2014), cell differentiation (Recknor *et al* 2006) and construction of artificial extracellular matrix (Bacakova *et al* 2004). A recent study has shown the sensing and adhesion machinery of cells can be controlled by surface patterning (Ventre *et al* 2014). Among the different techniques applied to modulate surface properties there has been increased attention on laser micromachining and, especially, on pulsed laser ablation (Bäuerle 2011). The laser ablation, with its single step process, has numerous advantages such as, high flexibility, direct patterning without the need for a resist process and also without the need for an etchant (Zhang *et al* 1998).

Graphene, a single atomic layer hexagonal lattice is considered to be a promising material exhibiting unique electrical, optical, thermal, and mechanical properties (Novoselov *et al* 2004, Geim and Novoselov 2007, Geim 2009). These intriguing properties have been exploited for several biomedical applications such as (Shao *et al* 2010, Hess *et al* 2013, Kakatkar *et al* 2015), drug delivery (Liu *et al* 2011) cancer therapies (Yang *et al* 2010) and neural interfacing (Hong *et al* 2014). The investigation of graphene which can be harnessed in an biomedical applications is asking for refined knowledge of the fundamental cell adhesion at the graphene interface, an important topic that remains less investigated. Among the different graphene species, single layer graphene (SLG) grown by chemical vapour deposition (CVD) may offer some advantages in the field of biosensor development: it can be easily transferred onto any other substrates, including flexible ones (Suk *et al* 2011); and it can be patterned (Park *et al* 2012, Strong *et al* 2012) for the creation of large area biosensors or devices. Nevertheless, up to date only a restricted number of investigations have addressed

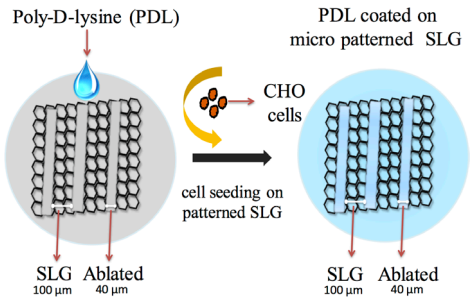

Figure 1. PDL coating on micropatterned substrate and CHO cell seeding.

the issue of cell coupling to SLG. In particular biocompatibility of SLG was studied employing osteoblasts and human mesenchymal stem cells (Kalbacova *et al* 2010); in a recent study, the cellular response of different graphene-coated substrates was investigated, showing that the underlying substrate effect might play an essential role in regulating adhesion and proliferation of cells like fibroblasts on these SLG-coated soft materials (Lin *et al* 2016). An investigation by our group (Lorenzoni *et al* 2013) showed the propensity of primary hippocampal neurons to adhere on SLG regions of patterned surfaces, giving the opportunity to create geometrically ordered neural networks; in the case of neurons, a layer of adhesion promoting poly-d-lysine (PDL) was necessary to allow cell adhesion and growth, otherwise hindered.

In view of the employment of CVD graphene as a biointerface, quantification of cell adhesion would be an ideal break through. To the best our knowledge, there was no approach used to quantify the cell adhesion graphene substrates. With the aim to explore the generality of cell adhesion phenomena onto the fabricated interface, we applied the same patterning technique and we studied the adhesion and growth of a different kind of eukaryotic cells, i.e. Chinese hamster ovarian (CHO) cells.

First, behaviour of CHO cells seeded onto PDL-coated micropatterned SLG substrates was monitored by time-lapse microscopy; confocal microscopy was employed on immunolabeled samples in order to obtain a more detailed investigation on the morphology and number of cells that were populating the two parts of the substrates. Further, single cell force spectroscopy (SCFS) was employed to quantify the adhesion of cells in the correspondence of graphene and ablated areas, respectively. The findings suggest that the fabricated PDL-coated micropatterned SLG favours the initial cell adhesion but, at a later time point, the topographical and chemical surface cues force the cells to migrate and move away from the SLG stripes, during the proliferation phase. This cell response is different from what previously observed with the hippocampal neurons (Lorenzoni *et al* 2013). This study escalates the understanding of the SLG interface with the living cells and, in particular, indicates that the response to the SLG interface is strictly cell-type dependent.

2. Materials and methods

2.1. SLG transfer

Commercially available CVD grown SLG on copper (Cu) (2D Tech, UK) was transferred by wet etching technique on Cu as follows. A layer of poly(methyl methacrylate) (PMMA) (MicroChem, 950 000 MW, 9–6 wt. % in anisole) was spin-coated (Sawatec SM-180-BT spinner) on one side of the SLG/Cu foils at 3000 rpm for 45 s; then, the SLG grown on the opposite side of the Cu foil was removed by 100 W oxygen plasma, followed by drying at room temperature for 12 h. The Cu was etched using 0.2 M ammonium persulphate (APS) solution in a Petri dish and the PMMA/SLG stack was floated on the surface of the solution. The stack of PMMA/SLG was carefully rinsed in Milli-Q (Millipore, 18 MΩ) to remove the traces of the Cu etchant, and then it was placed on the target substrate (14 mm glass coverslip). The transferred SLG substrate was annealed at 180 °C for 3 h for a firm adhesion to the glass coverslip and washed with acetone for the removal of PMMA. All the chemicals were from Sigma Aldrich. The quality of the SLG transfer was monitored by Raman spectroscopy.

2.2. Laser patterning of SLG

The transferred SLG was patterned by laser micromachining with micrometric resolution, following a protocol previously optimized and described (Lorenzoni *et al* 2013). Briefly, ablation patterning was performed by a KrF Excimer laser with 248 nm wavelength, exploiting the absorption peak of SLG in the deep UV at 4.6 eV. SLG on glass coverslip was patterned by exposure to series of single pulse at a fluence 0.5 J cm^{-2}; the patterns consisted of an array of vertical 100 μm wide stripes of SLG separated by 40 μm wide ablated stripes. The length of the stripes was 1000 μm.

2.3. Surface functionalization and cell culture

The CHO (ATCCs, CCL-61T,UK) cell lines were cultured in Dulbecco's modified eagle medium (DMEM) (Gibco, UK) containing 4.5% glutamine and glucose, 10% fetal bovine serum inactivated (FBS), 1% penicillin streptomycin (PS) and 1% non-essential amino acid (NEAA, Gibco, UK) at 37 °C with 5% CO_2.

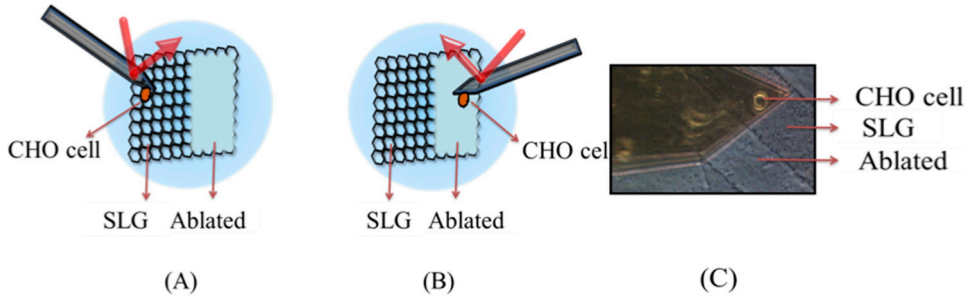

Figure 2. Adhesion points tested on PDL coated patterned substrates ((A) and (B)) and a CHO cell captured to an AFM cantilever (C).

The cells were split every 3–4 d, with a confluency rate of <80%.The patterned substrates were coated (figure 1) poly-d-lysine (Sigma m.w.70 000–150 000, 0.1 mg ml^{-1} in sterile water) for 3 h in an incubator (37 °C, humid atmosphere with 5% CO_2), and thoroughly rinsed with sterile deionized water.

2.4. Time lapse

Time-lapse experiments were performed for 72 h on a commercial bright field inverted microscope (Eclipse Ti E; Nikon Instruments Inc.) with laser-based autofocus. The microscope was equipped with a charge-coupled device (CCD) camera (Andor DU-897D-C00), 10 × objective and imaging software (NIS elements AR; Nikon Instruments Inc.). For long-term imaging, the coverslip with CHO cells was mounted in a closed chamber maintained at stable temperature 37 °C (TC-324B, Warner Instruments Corporation); to maintain the physiological pH, 5% CO_2 balanced with air was obtained by a flow meter (CO2 BX, Okolab) and injected in the chamber.

2.5. Immunostaining and confocal microscopy

The CHO cells were split when they reached 80% confluency and seeded on the PDL coated patterned substrates at a density of 210 cells mm^{-2}. Cells were fixed using 4% (w/v) Paraformaldehyde (PFA, SCBiotechnology, USA) in 1X PBS at different time intervals of 24 h and 48 h. The patterned substrates containing cells were washed once with pre-warmed PBS, pH 7.4 and fixed using 4%PFA for 10 min at room temperature. Each substrate was permeabilized with 0.1% Triton X-100 in PBS for 3–5 min. This was followed by adding 1% bovine serum albumin (BSA) to reduce nonspecific background staining with these conjugates. For selective F-actin staining the substrates were stained with 6.6 μM Alexa Fluor-647 phalloidin (life Technologies, USA) diluted in PBS 1X (1:40) and placed at room temperature for 20 min. After each step the substrates were washed with PBS 1X. Finally, the cells were air dried and then mounted on microscope slides by a permanent prolong anti-fade reagent with DAPI. The confocal analysis was finally carried out using a Nikon Inverted Microscope TiE equipped with a Nikon Confocal Laser System (Nikon Optical Co., Ltd, Japan) at an excitation wavelength $\lambda_{ex} = 405$ nm, and $\lambda_{ex} = 647$ nm.

2.6. Analysis of cell alignment

Images of the micropatterned cells were analysed using ImageJ software. The profile of each cell was fitted with an ellipse and cell orientation was denoted as the angle of the direction of the major axis of the ellipse and the direction of the stripes. At least a number of cell n = 200 was measured; the data are presented as the mean ± SD.

2.7. Single cell force spectroscopy

A Nanowizard III AFM system was used in combination with the CellHesion module (both from JPK instruments, Germany), which enables for an extended vertical displacement range of 100 μm. PDL coated patterned SLG substrates were attached with poly-dimethyl siloxane in Petri dishes customized with a central hole of 12 mm diameter, and mounted in the JPK Petri Dish Heater. Sample temperature was maintained constant at 37 °C. Single beam silicon tipless cantilevers TL1 with a nominal spring constant of 0.03 N m^{-1} (Nano And More, Germany) were functionalized with Concanavalin A (ConA, Sigma, USA), following the same procedure previously described (Canale *et al* 2013). The actual spring constant of each cantilever was determined *in situ*, using the thermal noise method.

For SCFS experiments the CHO cells were plated at an appropriate density of 3 × 10^3cells ml^{-1} in a standard sterile 35 mm Petri dish. The culture medium was removed from the Petri containing the confluent cells and the cells were washed with sterile phosphate buffered saline (PBS) and detached from the Petri dishes with a mild treatment of trypsin/ EDTA (Gibco,UK) solution at 37 °C for 2 min. The trypsinized cells in suspension were placed in 1 ml of culture media, centrifuged at 1200 rpm, resuspended again in PBS (with 2 mM $CaCl_2$ and 2 mM $MgCl_2$), and agitated for approximately 10 min before starting the measurements.

A small amount of cells was first injected in the AFM liquid chamber; using the optical microscope (AxioObserverD1, Zeiss, Germany) the cantilever was positioned over one cell and gently brought into contact with the cell with a controlled force of 2 nN for 30 s. The cell was raised from the surface for 15 min to firmly

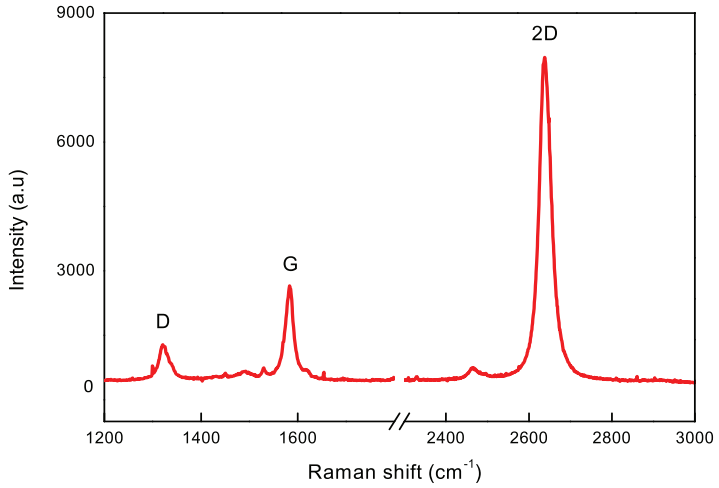

Figure 3. Raman analysis of SLG—Raman spectrum indicating the D, G and 2D peaks of SLG transferred onto a glass coverslip.

attached to the cantilever and then moved above the patterned area substrate. Cell adhesion was measured placing the cell in contact with different points of the PDL coated patterned substrates using the same force contact of 2 nN and keeping the adhesion time constant to 3 s. The velocity of the cantilever vertical displacement was set to 5 μm s^{-1} and the force curve length was set to 80 μm in order to achieve a complete cell detachment for each force–distance cycle. The experiments were performed in PBS with the addition of 2 mM $CaCl_2$ and 2 mM $MgCl_2$. The system was left for 10 min before the acquisition of every set of force spectroscopy curves. The collected force–distance curves were processed by JPK Data Processing and the data were analysed with OriginPro9.1. A sketch of the experiment is reported in figure 2, along with an optical image that shows a single CHO cell attached to the AFM cantilever standing on a SLG stripe.

2.8. Quantitative imaging

The adhesion of PDL-coated SLGs substrates was investigated by using a Nanowizard III AFM system (JPK Instruments) in the quantitative imaging (QI) mode. An Axio ObserverD1 inverted optical microscope (Carl Zeiss, Germany), coupled with the AFM system, was used to choose the areas for the mechanical analysis. V-shaped DNP silicon nitride cantilevers (Bruker, Billerica, MA, USA), with a nominal spring constant 0.24 N m^{-1}, the resonance frequency in the air in the 40–70 kHz range and tip typical curvature radius of 20–60 nm were used. The actual spring constant of each cantilever was determined *in situ*, using the thermal noise method. The acquisition of a large set of force–distance (FD) curves (128 × 128) was performed in PBS with maximum force load of 8 nN and curve length of 500 nm. QI images of 25 × 25 μm^2 were collected. The adhesive properties of the sample were extracted from the post-processing analysis of the acquired curves.

2.9. Raman spectroscopy

To evaluate the quality of the transferred SLG on 14 mm glass coverslip Raman spectroscopy were measured at ambient conditions using a Horiba Jobin Yvon LabRAM HR800 μRaman spectrometer equipped with a microscope. A 632.8 nm excitation line in backscattering geometry through a 50 × objective lens was used to excite the SLG on glass coverslip.

2.10. Wettability

To characterize surface wettability, water contact angle measurements (WCA) were performed with the sessile drop method using an optical contact angle measuring instrument (DataPhysics OCAH 200, Germany) at room temperature (RT). Each water droplet has a volume of 2 μl and was carefully touched to the sample surface at random locations to investigate the surface properties of PDL coated patterned SLG. The average contact angle values with the corresponding mean ± standard error of mean (SEM) were reported ($n = 8$ per sample).

2.11. Statistical analysis

The results are presented as mean ± SEM, unless otherwise mentioned. Statistical analyses were performed using SigmaPlot (Systat) and OriginPro 9.1 (OriginLab) software. Where appropriate, the statistical significance was assessed using student's *t*-test and one-way repeated measures ANOVA.

3. Results and discussion

3.1. Raman characterization

Raman spectroscopy was used to evaluate the quality of SLG transferred on the glass coverslip. To avoid the sample damage/heating the optical power was kept minimum at 613 μW. A typical Raman spectra obtained from a transferred SLG onto a glass coverslip is reported in figure 3. The Raman spectra has two intense features at ~1584 cm^{-1} ('G' band) due to the sp^2 vibration

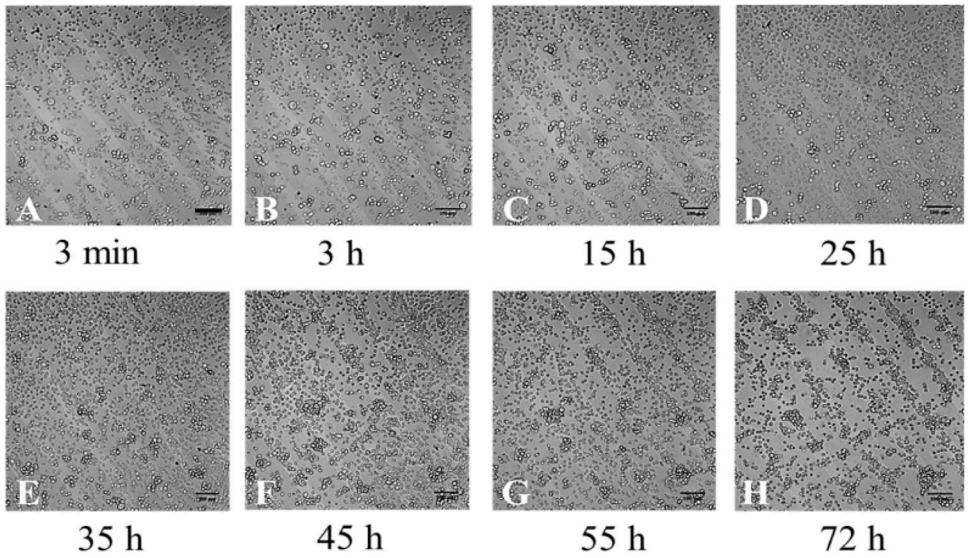

Figure 4. Time lapse optical images at different time interval of patterned PDL-SLG/ablated during migration of CHO cells (A: 3 min; B: 3h; C: 15h; D: 25 h; E: 35 h; F: 45h; G: 55h; H: 72h). The scale bar indicates 100 μm.

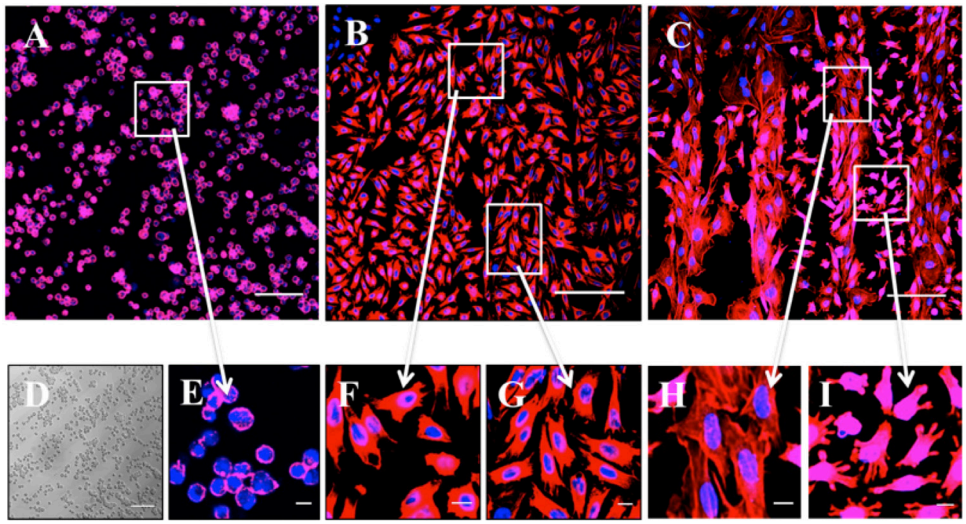

Figure 5. Morphological Images of CHO cells on PDL coated patterned SLG substrates: Immunofluorescence staining for DAPI in blue (nuclei) and phalloidin in red (actin filaments); morphology of cells (A)–(C) at 20 × magnification obtained after 3 h, 24 h and 48 h of culture, respectively. The scale bar indicates 100 μm (D) optical micrograph at 3 h indicating cells preferential adhesion on PDL coated—SLG. Figures ((E), (G) and (I)) and ((F) and (H)) magnified images of SLG and ablated region respectively. The scale bar indicates 10 μm.

and stronger single Lorentzian sharp peak centred around ~2700 cm^{-1} ('2D' band) of the SLG on the glass coverslip. A small 'D' peak, indicative of defects, was visible at ~1350 cm^{-1} (Ferrari *et al* 2006). The ratio of the intensity of the 2D peak to G peak (I_{2D}/I_G) is typically ~3 which indicated that SLG transferred on the glass coverslip still retained its properties, with low presence of defects.

3.2. CHO cell migration

3.2.1. *Time lapse*

To evaluate the CHO cell response onto the PDL coated patterned SLG-ablated substrates, the sample was observed under a microscope equipped with a cell incubator. The cell incubator system allowed the continuous long-term monitoring up to 72 h. Figure 4 displays eight frames of the time lapse video at different time from 3 min up to 72 h after cell seeding. Graphene stripes (100 μm width) appear slightly darker than ablated stripes (40 μm width). The time sequence clearly demonstrates that there is a rearrangement of CHO cells on the surface during time. In the figure 4 up to 25 h ((A)–(D)) the cells density is higher on the 100 μm wide SLG in comparison to the 40 μm wide ablated stripes, but, at around 35 h (figure 4(E) it was observed that cells slowly migrate towards the

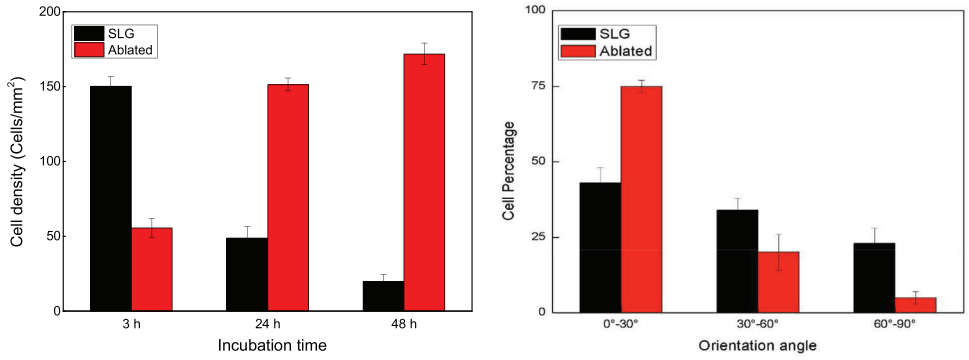

Figure 6. (A) CHO cell count on PDL-coated substrates of patterned SLG. (B) Cell orientation on the ablated and SLG stripes.

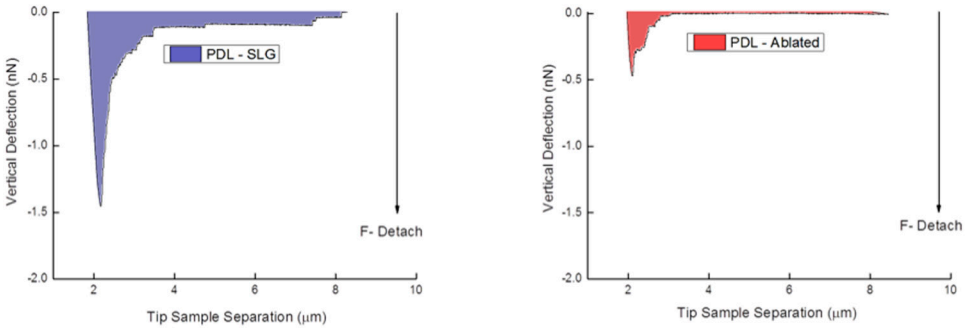

Figure 7. Typical force–distance curves acquired on PDL-coated SLG and ablated substrates.

ablated region, where they proliferate. At the end of 72 h (figure 4(H) the density of the cells was higher on ablated region, due to the combined effect of migration and proliferation. The complete time-lapse video taken during 72 h incubation of CHO cell on the patterned PDL-SLG/ablated substrate is available as supplementary information (stacks.iop.org/TDM/4/025022/mmedia).

3.2.2. Confocal microscopy on immunolabeled samples

The behaviour of CHO cells cultured on PDL coated SLGs was further investigated by confocal microscopy on immunolabeled samples. Figure 5 summarizes the findings. First of all, we confirmed the results of the time-lapse video, and we observed a re-arrangement of the cells at the surface over time. To quantify the cell density variation we exploited the DAPI fluorescence that clearly indicates the presence of cell nuclei, we counted the cell density in the two different areas of the sample, corresponding to SLG and ablated regions respectively. A summary of the CHO cell counts performed by nuclei DAPI staining and the subsequent analysis of the resulting images by means of the free software ImageJ 1.42v (USA) is displayed in figure 6(A). It was found that initially (3 h after) the cell density is higher on the graphene stripes (150 ± 7 cells mm^{-2} on SLG and 55 ± 6 cells cm^{-2} on ablated SLG). The scenario changed completely after 1 d *in vitro* (figure 6): CHO cells migrated towards the ablated region (49 ± 8 cells mm^{-2} on SLG and 151 ± 5 cells cm^{-2} on ablated SLG). The number of cells on SLG is still lower after 48 h (20 ± 5 cells mm^{-2} on SLG and 171 ± 7 cells cm^{-2} on ablated SLG), while, at the same time, the number of cells on the ablated region is still increased, as the consequence of migration and proliferation. After ~28 h the 40 μm wide ablated region was entirely covered with the cells.

From a morphological point of view, the actin staining shows that 3 h after seeding, CHO cells, almost exclusively placed onto SLG, were still round and not well spread, as expected in the initial adhesion phase (figures 5(A) and (E)). At a later time point (24 h) the cells were present on both areas, and they appeared well attached to the surface, with no clear difference in morphology. Finally, at 48 h, CHO cells were preferentially placed onto the ablated stripes, where they were in a proliferation phase: the cytoskeleton was well visible and stretched, cells presented the typical fibroblast shape, and it was noted that they were elongated along the pattern. On the contrary, few CHO cells were still present on graphene surface and showed an irregular morphology, with many membrane protrusions; additionally, all cells were isolated, with no contact point between each other. We quantified cell orientation along the stripes at DIV 2 and the results are summarized in figure 6(B). The bar graph clearly indicates that on the ablated stripes the vast majority

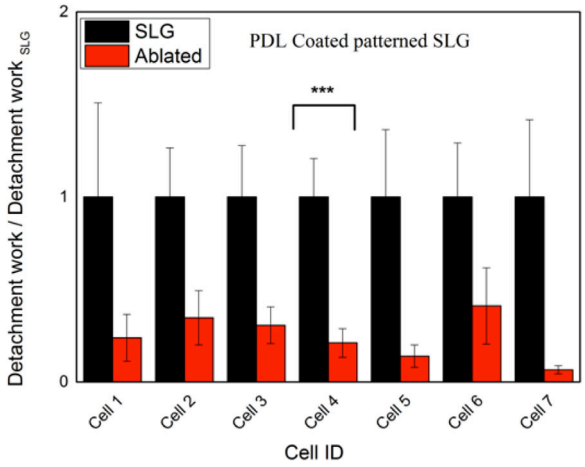

Figure 8. W_{detach} on SLG and ablated regions normalized with respect to the values obtained on SLG. For each bar, $n > 15$. The detachment work was significantly lower on ablated regions for all cells ($P \leqslant 0.001$; student's t-test).

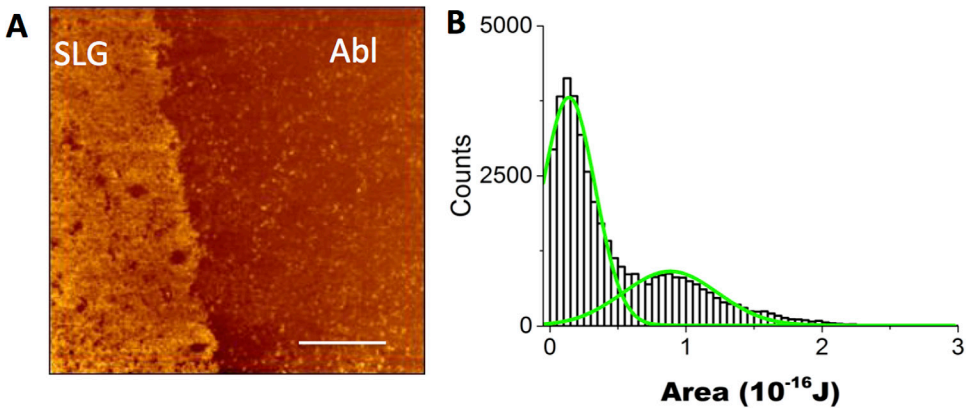

Figure 9. Adhesion map obtained in QI mode (A). The adhesion is higher in correspondence of the SLG stripe. Scale bar, 5μm; data scale, 5 nN. (B) Distribution of the adhesion work calculated per each curve of the map in (A). Two distinct populations are present and here fitted with Gaussian curves, centred at 1.2×10^{-17} J and 8.8×10^{-17} J respectively.

of cells (75%) are aligned with the stripe direction; on the contrary on SLG no preferential orientation was observed.

3.3. SCFS measured adhesion

The quantification of the CHO cell adhesion on the PDL-coated patterned SLG was done by means of SCFS. The adhesion of a single cell was sequentially tested on different points chosen with the aid of the optical images on both the types of substrates with the same cell. This allows the comparison of the detachment works measured on the two different surfaces. Figure 7 shows the typical retraction part of two force–distance curves acquires on SLG and on ablated region respectively. The total area delimited by the part of the retracted curve below the FD curves baseline, respectively in blue and in red in figure 7, provides the evaluation of the detachment work (W_{detach}), i.e. the physical quantity that we take into account to characterize the adhesion properties of cells on the two parts of the patterned substrate.

Figure 8 shows W_{detach} measured for 7 different CHO cells by using the same experimental parameters. The values shown in figure 8 derived from the average of the results obtained on at least 15 different adhesion points per each cell, normalized with respect to the quantity measured on SLG. In all the cases, cells were adhering more on the SLG stripes with respect to the ablated regions, the differences are statistically significant for all the cells (t-test $P \leqslant 0.001$).

It is worth noting that both SLG and ablated region are PDL coated and, therefore, chemically identical; in order to elucidate the reason of the different cell behaviour at the two surfaces, we performed a quantification of adhesion properties of the interface by quantitative imaging. In this experiment the detachment work of the AFM tip from the surface is quantified. The results indicated indeed a significant contrast in this physical parameter, as shown in the adhesion map reported in figure 9(A). The adhesion was higher in correspondence of the SLG stripe. In the scanned region, at the boundary between SLG and ablated areas, two distinct populations of detachment work were present, centred at 1.2×10^{-17} J and 8.8×10^{-17} J, in ablated and SLG region, respectively. Clearly, the PDL polymer arranges

differently on SLG with respect to the ablated part, possibly exposing a larger number of charged groups on its surfaces and providing a larger number of binding sites to the cell membrane.

4. Discussion

In our previous work (Lorenzoni *et al* 2013) we worked on the same types of PDL-coated SLG patterned substrates and it was demonstrated that hippocampal neurons were able to grow selectively on the SLG stripes of the pattern, avoiding the ablated regions. In the case of neurons, the interface between graphene and neural cells was considered extremely advantageous for exploring and stimulating their electrical behavior. On the other hand, the chemical stability of graphene could also be exploited for tissue regeneration. The possibility to grow ordered geometry of cell *in vitro* could be very appealing for some applications, such as biosensor development or tissue engineering. However, the results obtained on neural cells cannot be extended to other kind of cells without further investigation. The aim of this second work was to understand if the adhesion and growth on SLGs patterned substrates obtained via ablation could be generalized to other cell types. Therefore, we extended our method tested on neurons to a different cell line, which could give us the opportunity to quantify cell adhesion, as well. The small size of neural cells and their delicateness ruled out the possibility to carry out SCFS measurements with primary neurons. In the first pioneering work, the images and the video supported the hypothesis that neurons could anchor very strongly on the PDL-coated SLG surface and they were pulled onto SLG from the adjacent ablated SLG stripes, after connections between them had been built. In the initial adhesion phase (i.e. at a time point directly comparable to the SCFS measurement) a higher cell density of CHO cells was shown onto PDL-SLG stripes in the time lapse and the immunofluorescence images (figures 4(A), 5(A) and (D), respectively). The result is consistent with the observation made on the hippocampal neurons. However, once the adhesion phase was completed, the CHO cell response to the surface properties forced them to migrate towards the adjacent graphene-ablated regions; the migration was accompanied with an evident change in morphology of the cells, which appeared very well stretched onto the ablated substrate; additionally, the pattern induced an orientation along the direction of stripes. The elongation of cells along the stripe direction is an effect of the pattern geometry. In fact, it has been shown (He *et al* 2014, 2015) that substrate geometry dramatically influence cell-matrix and cell-cell interaction, inducing pattern-dependent collective arrangement of cells. In particular, in our case the narrow width of the ablated stripes (40 μm), comparable to cell dimension, induce a complete elongation in the direction of the stripes, since all the CHO cells on the ablated areas are in contact with the boundary region. On the contrary, on SLG, the sparse cells remaining on graphene at DIV2, do not feel the geometric constraint imposed by the underlying interface, and, therefore, do not show any particular orientation. This result is also related to the question on how far cells can sense their microenvironment and it is in good agreement with the literature setting in 100 μm the threshold for mechanosensing. With the aim to unambiguously quantify the adhesion properties of single CHO cells on PDL-coated substrates of patterned SLG, we employed SCFS as described in the Materials and Methods section. The superior cell binding efficiency of PDL-SLG was clearly evidenced by SCFS measurements (figure 8), since W_{detach} calculated for 7 different probe cells showed higher values on PDL-coated SLG on each of the 7 independent trials carried out. The values of WCA measured with the sessile drop method on PDL-SLG ($50° \pm 2°$) and PDL-ablated ($85° \pm 1°$) was performed to investigate the surface properties patterned substrates. The difference in wettability between the two surfaces explains fairly well this finding: CHO cells adhere more strongly onto a more hydrophilic surface, which exposes a higher number of binding sites. In spite of the fact that the substrate is uniformly coated with PDL, different physico-chemical properties characterize the two regions, probably due to a different molecular arrangement of the polymer on the SLG with respect to the ablated region. Beside wettability, QI measurements performed on the PDL-coated pattern evidenced an adhesion contrast of the two regions, as shown in the adhesion maps and quantified by the detachment work. Therefore, in spite a uniform chemical coating, differences in cell behaviour are originated from the substrate itself (SLG versus ablated part). We envisaged that the different structure of the materials indirectly influence the cell-matrix interaction and therefore have a role in size and number of focal adhesions on SLG with respect to ablated part, resulting in the migration of CHO towards the ablated areas. It is indeed well-known that the micro- and nano- structure of a surface influence cell grow and migration (Arnold *et al* 2004, He *et al* 2015), by tuning the dimension of focal adhesions clusters. This issue is now subject of further investigation.

5. Conclusion

In this investigation the use of micropatterned SLG for the obtainment of geometrically ordered CHO cell cultures was demonstrated. CHO cells were shown to behave dynamically, by adhering first onto the SLG areas, and then migrating onto the adjacent SLG ablated stripes, which were more favourable to proliferation. The resulting cell arrangement was different from that obtained with primary neurons. Therefore, this investigation clearly demonstrates that the response to identical surface cues (topographical and chemical) is a cell-type dependent mechanism; the interplay

between these two factors, i.e. surface properties and specific cell response, need to be taken into account whenever planning a surface functionalization for applicative purposes. This work supported the idea that different patterning techniques must be accurately tailored for biosensors or biomedical application that have different cells/tissues as final targets. This cell-type dependent behaviour may be caused by several factors, ranging from the different properties of the cell membranes to the differences in the overall cell functionality, and it deserve further investigation.

Further, in this work, we quantified the phenomena of cell adhesion by SCFS using single CHO cells as probes and testing their adhesion on PDL coated patterned substrates. To the best of our knowledge, this is the first time that this technique is applied to quantify cell adhesion on graphene. Interestingly, the results indicate a higher adhesion on the PDL-coated SLG stripes, with respect to the adjacent ablated stripes, suggesting that the properties of the underlying substrate (i.e. SLG) affect the adhesion layer (PDL) and, as a consequence of it, the adhesion machinery of the cell is also influenced.

References

Arnold M *et al* 2004 Activation of integrin function by nanopatterned adhesive interfaces *ChemPhysChem* **5** 383–8

Bacakova L *et al* 2004 Cell adhesion on artificial materials for tissue engineering *Physiol Res.* **53** S35–45

Canale C *et al* 2013 A new quantitative experimental approach to investigate single cell adhesion on multifunctional substrates *Biosens. Bioelectron.* **48** 172–9

Bäuerle D W 2011 *Laser Processing and Chemistry* vol 208 (Berlin: Springer) pp 291–2

Ferrari A C *et al* 2006 Raman spectrum of graphene and graphene layers *Phys. Rev. Lett.* **97** 187401

Geim A K 2009 Graphene: status and prospects *Prospects* **324** 1–8

Geim A. K and Novoselov K S 2007 The rise of graphene *Nat. Mater.* **6** 183–91

He S *et al* 2014 Some basic questions on mechanosensing in cell-substrate interaction *J. Mech. Phys. Solids* **70** 116–35

He S *et al* 2015 Dissecting collective cell behavior in polarization and alignment on micropatterned substrates *Biophys. J.* **109** 489–500

Hess L H, Seifert M and Garrido J A 2013 Graphene transistors for bioelectronics *Proc. IEEE* **101** 1780–92

Hong S W *et al* 2014 Enhanced neural cell adhesion and neurite outgrowth on graphene-based biomimetic substrates *BioMed. Res. Int.* **2014** 212149

Jeon H J, Simon C G and Kim G H 2014 A mini-review: cell response to microscale, nanoscale, and hierarchical patterning of surface structure *J. Biomed. Mater. Res.* B **102** 1580–94

Kakatkar A *et al* 2015 Detection of DNA and poly-l-lysine using CVD graphene-channel FET biosensors *Nanotechnology* **26** 125502

Kalbacova M *et al* 2010 Graphene substrates promote adherence of human osteoblasts and mesenchymal stromal cells *Carbon* **48** 4323–9

Lin F *et al* 2016 Substrate effect modulates adhesion and proliferation of fibroblast on graphene layer *Colloids Surf.* B **146** 785–93

Liu K *et al* 2011 Green and facile synthesis of highly biocompatible graphene nanosheets and its application for cellular imaging and drug delivery *J. Mater. Chem.* **21** 12034–40

Lorenzoni M *et al* 2013 Simple and effective graphene laser processing for neuron patterning application *Sci. Rep.* **3**

Novoselov K S *et al* 2004 Electric field effect in atomically thin carbon films *Science* **306** 666–9

Park J B, Yoo J H and Grigoropoulos C P 2012 Multi-scale graphene patterns on arbitrary substrates via laser-assisted transfer-printing process *Appl. Phys. Lett.* **101** 043110

Recknor J B, Sakaguchi D S and Mallapragada S K 2006 Directed growth and selective differentiation of neural progenitor cells on micropatterned polymer substrates *Biomaterials* **27** 4098–108

Shao Y *et al* 2010 Graphene based electrochemical sensors and biosensors: a review *Electroanalysis* **22** 1027–36

Strong V *et al* 2012 Patterning and electronic tuning of laser scribed graphene for flexible all-carbon devices *ACS Nano* **6** 1395–403

Suk J W *et al* 2011 Transfer of CVD-grown monolayer graphene onto arbitrary substrates *ACS Nano* **5** 6916–24

Ventre M *et al* 2014 Topographic cell instructive patterns to control cell adhesion, polarization and migration *J. R. Soc. Interface* **11** 20140687

Yang K *et al* 2010 Graphene in mice: ultrahigh *in vivo* tumor uptake and efficient photothermal therapy *Nano Lett.* **10** 3318–23

Zhang J, Sugioka K and Midorikawa K 1998 Direct fabrication of micrograting in fused quartz by laser-induced plasma-assisted ablation with a KrF excimer laser *Opt. Lett.* **23** 1486–8